RESULTS OF BLOWOUT REGIME PROPAGATION EXPERIMENTS OF AN ELECTRON BEAM IN A PLASMA

N.Barov[1], M.Conde[2], W. Gai[2] and J.B.Rosenzweig[1]
[1]Dept. of Physics and Astronomy, UCLA, 405 Hilgard Ave., Los Angeles, CA 90095
[2]Argonne National Laboratory, 9700 S.Cass Ave., Argonne IL 60439

I. INTRODUCTION

When a tightly focused electron beam propagates in an underdense plasma (beam density greater than the plasma electron density, $n_b > n_0$), the plasma electrons are expelled radially by the space-charge of the beam, forming an ion channel which in turn provides a uniform, linear focusing force on the beam. When the beam is short ($\sigma_z < 2k_p^{-1}$), making it suitable as a driver for plasma wake-field acceleration (PWFA)[3], requirements on the beam properties (current, eminence and energy) to achieve ion channel self-focusing become more difficult to satisfy[10]. If the beam is initially β-matched to the focusing gradient, that is, the β-function is initially equal to $\beta_{eq} = \sqrt{\gamma / 2\pi r_e n_0}$, where σ_r and ε, are the rms transverse beam radius and emittance, the transverse distribution in the body of the beam is nearly stationary, while that near the head expands radially. The loss in beam density near the head associated with this expansion further retards the plasma electron response and causes the pinch point (where sufficient focusing gradient develops) to move backwards in the beam frame. The fast relaxation distance for these beam head dynamics is roughly $4\beta_{eq}$, or 5 cm for our experimental conditions, which is less than half of the plasma length, $L_p = 12$ cm.

The present experiments were motivated by the proposed use of the underdense regime as the basis for a PWFA[8] (the blowout regime) which is very attractive in terms of drive and accelerating beam guiding, in that when a plasma-electron free ion column is formed, the focusing force in this region is linear and the acceleration gradient is independent of radius.

II. EXPERIMENTAL SETUP

The plasma chamber used in the experiments is shown in Fig. 1, with 14.5 MeV electron pulses derived from the Argonne Wakefield Accelerator (AWA)[14] entering from the left. Beam diagnostics immediately upstream of the plasma chamber include an energy spectrometer, an emittance measurement system, an integrating current transformer (ICT) and Faraday cup to measure Q, a phosphor screen and at the focal point of the β-matching solenoid, an optical transition radiation (OTR) screen to obtain transverse beam profile images.

The plasma is created by a DC hollow cathode arc discharge, running at 55 V and 40 A, with Ar gas fed between concentric tantalum tubes. The (approximately 25% ionization fraction) plasma density, which is in the region of $n_0 = 1.15 \times 10^{13}$ cm^{-3}, is mapped with a cylindrical Langmuir probe (calibrated with a 140 GHz microwave interferometer), and found to be within 10 percent of the peak value over the nominal plasma length, $L_p \cong 12$ cm, with a steep initial ramp near the cathode tip. The half-maximum point, located 9 mm downstream of the cathode, is 12.25 cm away from the diagnostic-filled anode.

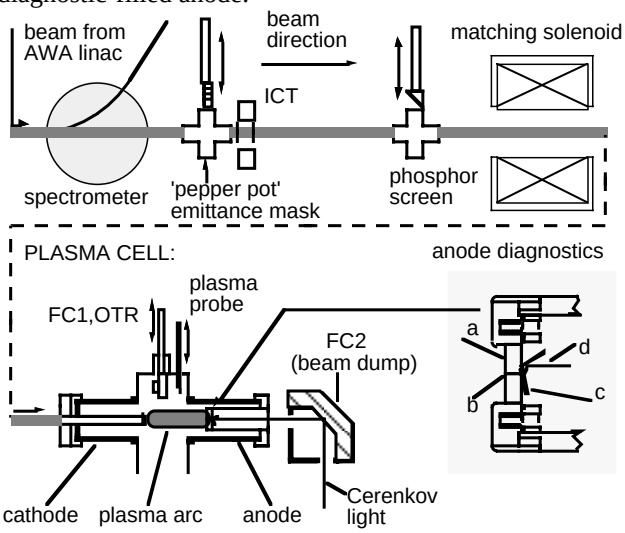

Fig. 1 Diagnostics beamline and plasma cell (shown without the plasma radial confinement solenoid). The anode diagnostics include (a) tungsten collimator with (b) 1 mm wide slit, (c) 500 μm thick quartz Cerenkov radiator, and (d) mirror and outgoing light.

III. EXPERIMENTAL RESULTS

The bunch charge Q was measured for every shot using the nondestructive integrating current transformer (ICT). Prior to this, the small fraction of charge scraped at the cathode assembly aperture must be quantified with simultaneous measurements with the ICT and FC1, the Faraday cup following the cathode. The focal spot size near the waist of the β-matching solenoid was measured with the OTR screen at FC1. Some of these profiles deviated significantly from the cylindrical symmetry assumed in the simulations; the shots characterized by an ellipse with an aspect ratio higher than 2:1 (25% of the population) were discarded. The remaining images were tested for peak intensity as well as for fractional integrated intensity inside a test radius of 0.28 mm. A symmetric Gaussian with $\sigma_x = \sigma_y = \sigma_r$, having the same integral defines an effective radius, which was found to be nearly independent of Q, with mean value of $\sigma_r = 284 \pm 24$ μm. The presence of shots

0-7803-4376-X/98/$10.00 © 1998 IEEE

with mild eccentricities causes the effective Gaussian profile to underestimate the peak beam density, predicting n_b / n_0=2.0 at 14 nC (this assumes a 25 psec FWHM bunch length). The actual value from the peak intensity in the image data is n_b / n_0=2.0 and 2.5 at Q=7 and 14 nC, respectively. The plasma is therefore well underdense at beam input for all experimental conditions. The beam divergence $\sigma_{x'}$ and bunch length were measured using the anode diagnostics, including a 1-mm wide (and 4 mm deep) tungsten slit aperture followed by a 0.5 mm thick Cerenkov emitter inclined 12 degrees to the beam direction. The light is sent to either a CCD camera for time-integrated imaging or to the 2 psec resolution streak camera. The beam charge after collimation by the slit aperture is measured at the Faraday cup following the anode, FC2. The beam divergence $\sigma_{x'}$, is sampled by recording the transverse profile along the slit after it has drifted $\cong 12$cm, and fitting a Gaussian. The beam divergence is 18.5 mrad at 14 nC and decreases linearly to 15.5 mrad at 7 nC, yielding $\varepsilon_n = 149$ and 130 mm-mrad and initial β_i=1.52 and 1.74 cm, for high and low charge, respectively. The *b*-function in these cases is only slightly mismatched to the ion focusing $\beta_{eq} = 1.25$ cm. The input bunch length is measured by refocusing the beam on the anode, with the Cerenkov light analyzed using a Hammamatsu C1587 streak camera; the bunch length is found to be 25 ± 3 psec FWHM.

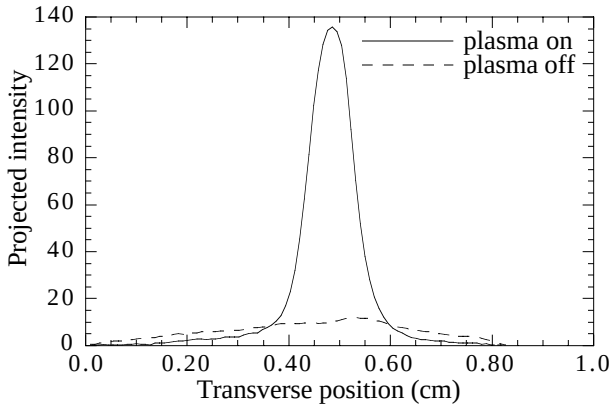

Fig. 2 Transverse beam profile after collimation, from digitized CCD camera image of Cerenkov light.

After the beam is collimated, the transmitted charge Q_{tr} is recorded on the downstream Faraday cup FC2. With plasma focusing, a substantial fraction, $\eta = Q_{tr} / Q$, of the initial charge ought to be transmitted through the slit, serving as an independent measure of the beam radius. With the plasma arc on, the downstream Cerenkov profile, as shown in Fig. 2, displays a narrow, intense peak as a result of ion focusing. The x-projected FWHM of a typical case (Fig 5) is 0.9 mm, 40% broader than at the start of the plasma, but consistent with the radial spreading at the beam head predicted by simulations, and markedly different than the no-plasma background. As the beam's transverse centroid jitter is significant on the scale of the slit aperture, shots with the y-peak too close to one of the aperture edges were rejected. The values of η selected in this way for an initially matched ($z_0 = 0$) case are displayed in Fig. 3 along with the results of simulations, as explained below. The low-η data points, especially at low Q, are thought to result from beam conditions differing from cylindrical symmetry, one possibility being a beam with a double-peaked y-profile starting from irregular initial conditions. Some of the spread in the data also undoubtedly comes from fluctuations in the initial beam aspect ratio, which give rise to quadrupole as well as monopole beam motion.

The simulation results given in Fig. 3 use the plasma fluid code NOVO[7], modified to include a super-particle representation of the beam electrons as described in [9]. The results of this code have been benchmarked against an electromagnetic particle-in-cell (PIC) code; the calculation of transmission efficiency is nearly the same, being smaller in NOVO by 4%, and so NOVO was employed for this analysis because of its speed. The calculations use 8000 beam particles, initialized to a thermal distribution derived from the measured beam size and divergence.

A more detailed view of the underlying dynamics is offered by the time-resolved streak camera analysis. These images contain information only about longitudinal and horizontal profiles, as measured in a 20 μm vertical strip in the center of the slit aperture. The beam was determined to be adequately vertically centered in this measurement by requiring $\eta \geq 0.45$. A streak image obtained in this way is shown in Fig. 4, displaying the predicted flaring of the distribution outward at the beam head.

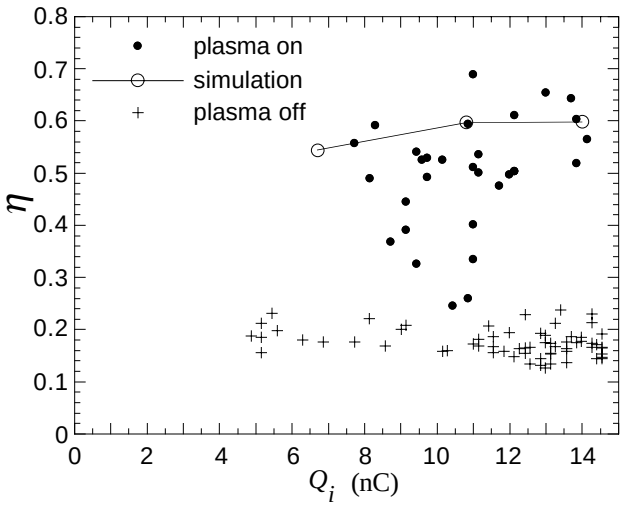

Fig. 3 Transmission data and simulations for an initially nearly β-matched case.

Each image that was analyzed further was sliced into short (5.7 psec) *t*-sections, and for every *t*-slice the integrated (in *x*) intensity, and a measure of the beam width defined by the region $-x_{1/2} \leq x \leq x_{1/2}$ containing half the integrated intensity were determined. The results of this analysis for 10 images within narrow input charge window ($10.2 < Q < 11.8$ nC) were summed to produce a composite picture of the beam distribution,

shown in Fig. 5, along with the accompanying rms error and PIC simulation results, analyzed to give beam width as a function of *t*-slice. The experimental data and PIC simulations clearly display a profile flared at the beam head due to radial expansion, as well as a beam core which is nearly matched and slightly larger, $\sigma_r \cong 370\ \mu$m, than at input. The simulation's agreement with the data is quite good, with a notable deviation in that the experimental results show less pronounced beam head expansion. This may be due to the assumption of a beam with a thermal input transverse phase space, which is not strictly correct for a photoinjector-derived beam, where the emittance of a single *t*-slice of the beam is smaller than the full beam[16].

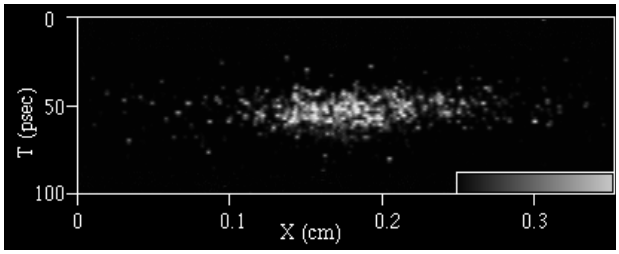

Fig. 4. Streak camera image of plasma exit beam profile.

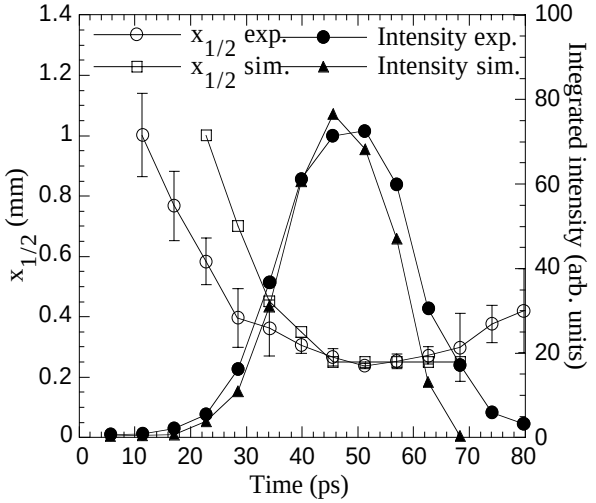

Fig. 5 Time-slice dependence of beam intensity and half-width, from experiment (exp.) and PIC simulation (sim.).

IV. CONCLUSIONS AND FUTURE WORK

In conclusion, short intense relativistic bunches, of the kind available from rf photoinjectors, have been observed, through integrated and time-dependent imaging, as well as collimator transmission, to effectively self-guide in an underdense plasma over many times the initial β-function. Picosecond-resolution measurement of transverse beam size displays the trumpet-shaped beam head predicted by simulations and analysis[10,11]. The simulations are in good quantitative agreement with the beam sizes and transmissions obtained from experiment, with deviations arising from the approximations involved in the simulation model of the beam.

In the next round of experiments, starting June '97, we plan to use a very similar set of experimental conditions to demonstrate high gradient acceleration in a PWFA, by measuring the energy changes of a witness beam propagating in the wake-field of the more intense drive bunch. The beam diagnostics developed for the present work, together with recent improvements to the AWA facility ($\cong$18 ps FWHM bunch length for Q=90 nC [18]), will greatly facilitate the measurement of high-gradient wake-fields. The peak acceleration gradient predicted for this experiment is in the range of 80 to 150 MeV/m, much higher than an earlier experiment at the AWA[9], which yielded 4 - 10 MeV/m. To measure this, we plan, like in the earlier experiment, to generate the witness beam in the same photocathode cavity as the drive beam[9], but additionally to time-resolve the final energy distribution of both beams using the streak camera. This strategy is necessary to overcome the 'shadow' effect occurring when the drive and witness beams overlap in energy.

ACKNOWLEDGMENTS

The authors would like to thank E. Colby, A. Murokh, P. Schoessow and J. Simpson for aid and advice along the way. This work supported by U.S. Dept. of Energy grants DE-FG03-93ER40796 and W-31-109-ENG-38, and the Alfred P. Sloan Foundation grant BR-3225. A more detailed account of this work has been submitted to Physical Review Letters under the title "Propagation of Short Electron Pulses in a Self-formed Ion Channel".

REFERENCES

[1] W.E. Martin, *et al*, *Phys. Rev. Lett.* **54**, 685 (1985).
[2] P. Chen, *et al*, *Phys.Rev.Lett.* **54**, 693 (1985), J.B.Rosenzweig, *et al.*, *Phys.Rev.Lett.* **61**, 98 (1988).
[3] G.Hairapetian, *et al*, *Phys.Rev.Lett.* **72**, 1244 (1994), H. Nakanishi, *et al.*, *Phys.Rev.Lett.* **66**, 177 (1991).
[4] B.N.Breizman, T.Tajima, D.L.Fisher, and P.Z.Chebotaev (unpublished).
[5] J.B.Rosenzweig, *et al.*, *Phys.Rev.A* **44**, R6189 (1991).
[6] N. Barov, *et al.*, *Proc. 1995 Particle Accelerator Conference*, 631 (IEEE, 1995).
[7] N. Barov and J.B.Rosenzweig, *Phys.Rev. E* **49**, 4407 (1994).
[8] J. Krall, *et al.*, *Phys. Fluids B* **1**, 2099 (1989).
[9] J. Krall and G. Joyce, in *Advanced Accel. Concepts* p.505 (AIP Conf. Proc. 335, 1995).
[10] P. Schoessow, *et al.*, *Proc. 1995 Particle Accelerator Conference*, 976 (IEEE, 1996).
[11] X. Qiu, *et al.*, *Phys.Rev.Lett.* **76**, 3723 (1996).
[12] J.Power, *et al.*: *Proc. of the 7th Workshop on Advanced Accelerators*, Lake Tahoe, CA (1996)
[13] M.E.Conde, et al.,These proceedings.